

Close range radar remote sensing of concrete degradation in a textile factory floor

H. Lorenzo ^{a,*}, V. Cuéllar ^b, M.C. Hernández ^c

^a *ETSE Minas, Universidade de Vigo, Campus Marcosende, 36280-Vigo, Spain*

^b *Laboratorio de Geotecnia, CEDEX, c / Alfonso XII, 3 y 5, 28014-Madrid, Spain*

^c *Facultad de CC. Físicas, Universidad Complutense de Madrid, 28040-Madrid, Spain*

Accepted 8 May 2001

Abstract

This paper describes a GPR study carried out with the aim of evaluating deterioration of concrete floors in a textile factory. In the past, production process waste was spilt onto the floor of the factory. A slow but continuous action from this waste on the concrete caused a significant variation in its porosity that can be detected by studying changes in the GPR reflected pulse. A simple synthetic model was developed in order to obtain information about how the response of the GPR antenna pulse is affected by changes in the porosity of concrete. It should also be taken into account the different conditions of the factory floor at the time of testing, as it had been isolated from the action of waste for many years. The heterogeneous conditions of the floor and the simplicity of the model used did not allow for an accurate estimate of the porosity; however, it was possible to map *degraded areas* of the floor in relationship to changes in the reflected signal. Core samples taken showed that some areas had concrete porosity of 15% and up to 25%, which is closer to that of sand than to concrete. © 2001 Elsevier Science B.V. All rights reserved.

Keywords: GPR; Remote Sensing; Radar; Concrete porosity

1. Introduction

Textile factories produce chemical waste and by-products during some of their production processes. An inadequate removal can cause problems not only in the environment but also within the factory itself. This was the situation in a factory, which had spilt liquid waste and by-products onto its 30-cm-thick concrete floor for a period of 15 years. This slow but continuous action of these waste products on the concrete was the cause of major deterioration in its internal structure.

In looking for a solution to this problem, the spillages were stopped and the top of the floor was covered with a new layer of small slabs. After this, a structural study of the concrete was carried out by taking core samples from some areas of the floor; this investigation indicated the effect of the liquid in the concrete, increasing its porosity especially within its first 15 cm.

This information allowed us to design a GPR investigation with the aim of detecting those areas of the floor that showed changes in their porosity. A synthetic model was developed in order to obtain information about the response of the GPR antenna pulse depending on the changes in the porosity of the concrete. The model is based on the following hy-

* Corresponding author. Fax: +34-986-813-644.
E-mail address: hlorenzo@uvigo.es (H. Lorenzo).

pothesis: the liquid attacks the concrete from top to bottom; this means that its effect could be seen more evidently just below the surface.

It was decided to study the reflection of the air–concrete interface because it would be representative of the condition of the concrete. To have a clear reflection of this interface, the 900-MHz antenna used was placed at a distance of 25 cm from the floor using a non-metallic, moveable skate.

As the floor had not been exposed to the liquid for some time, it was thought that the conductivity of the concrete would not be so high. Therefore, the variation of porosity should appear as a reduction in the reflection coefficient because of the decrease in the concrete dielectric constant.

Some radar tests were made where the core drills samples had been taken. The results indicated that soundings made near core sample areas where the porosity was high, showed changes in the reflection coefficient, in comparison to those made in sound concrete. Thus, a full GPR study of the factory floor was made, which allowed us to map those zones of “less reflection coefficient” associated with degradation in the concrete floor.

During the last 15 years, there has been a substantial amount of publication work where GPR is extensively used for non-destructive testing of civil engineering structures and to infer the electromagnetic parameters of a material, many of them through the study of the reflection coefficient. These works include advances in bridge deck control and evaluation (Carter et al., 1992; Weil, 1992; Chung et al., 1994; Halabe et al., 1997; Yelf and Carse, 2000), development of numerical methods to provide detailed information of the electromagnetic parameters and internal structure of pavement materials, (Halabe, 1990; Molineaux et al., 1995; Sousky et al., 1996; Lázaro-Mancilla and Gómez-Treviño, 2000; Olhoft, 2000; Shaw et al., 2000), characterization of materials under laboratory conditions (Shaw et al., 1993; Tsui and Matteus, 1997; Matthews et al., 1998; Robert, 1998; Shang et al., 1999), estimation of permittivity through the reflection coefficient (Glover, 1987; Maser and Scullion, 1991; Saarenketo and Roimela, 1998; Al-Qadi et al., 2000; Reppert et al., 2000).

Most of these works try to obtain the best appraisal of construction and pavement materials permittivity and conductivity, studying samples under

very controlled conditions (porosity, moisture content, etc.), and propose models and mixing laws to advance predicting changes in those parameters. In our case, the unknown variations of the internal structure of the floor cause problems in providing an accurate estimation of its porosity based on any of those models. The very dry condition of the floor allows us to apply a simple method to look for large variations in the concrete porosity based on variations in the reflection coefficient (which, in this special case, seems mainly to depend on its permittivity) between sound and degraded concrete.

2. Method

The study carried out with GPR endeavoured to evaluate the effect of an increase in concrete porosity in radar response, and check if this effect allows detection and mapping of high degradation areas.

2.1. Influence of porosity in the electromagnetic parameters of concrete

Based on the works of Cook (1975), Ulriksen (1982), Glover (1987), Halabe (1990), and also on recommendations of the ASTM Standard D4748-87, we accept a typical value of 6.2 for the real part of relative permittivity (ϵ'_r) of sound and dry concrete, and 10^{-2} – 10^{-4} mho/m for its conductivity (σ). Core samples taken from both sound and degraded areas showed porosity of 5% and 15–25%, respectively.

In Fig. 1, we see that for a frequency of 900 MHz and conductivity values of 10^{-2} mho/m or less, the contribution of σ in $\tan \delta$ (δ , loss angle) to obtain an estimation of impedance is negligible against its dependence from ϵ'_r .

The effect of porosity variation in the concrete dielectric constant ϵ'_r can be predicted through “Wiener formula” (Ulriksen, 1982). In accepting a concrete with a very slight degree of saturation (concrete pores just *full* of air), the formula simplifies to:

$$\frac{\epsilon'_{rc} - 1}{\epsilon'_{rc} + 2} = (1 - p) \left(\frac{\epsilon'_{rs} - 1}{\epsilon'_{rs} + 2} \right) \quad (1)$$

where ϵ'_{rc} = concrete relative permittivity, ϵ'_{rs} = solid matrix relative permittivity, p = porosity.

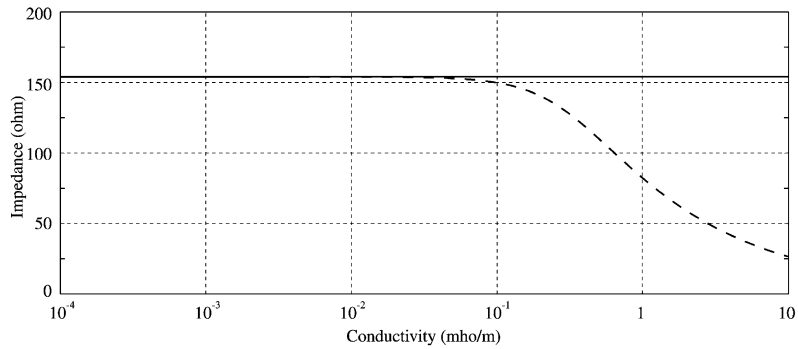


Fig. 1. Impedance as function of conductivity, at 900-MHz frequency, for a material with $\epsilon'_r = 6$. Dashed line: $\eta = (\mu/\epsilon)^{1/2}$. Solid line: $\eta = (\mu/\epsilon)^{1/2}/(1 + \tan^2\delta)^{1/4}$.

The special conditions of the floor—under cover of rain and free from liquid waste being spilt on it for many years—allows us to assume Eq. (1) without committing major errors.

Two more formulas were used to predict the variation of concrete permittivity. First, from Hara and Sakayama (1984), which results:

$$\sqrt{\epsilon'_{rc}} = p + (1 - p)\sqrt{\epsilon'_{rs}} \quad (2)$$

Second, from BHS formula—Olhoeft (1987), Duke (1990)—which results:

$$\frac{\epsilon'_{rs} - \epsilon'_{rc}}{\epsilon'_{rs} - 1} = p(\epsilon'_{rc})^{1/3} \quad (3)$$

Fig. 2 is the plot of these three formulas. They show the theoretical evolution of concrete permittivity according to porosity increase (we use a simple

model as an example that serves to show the internal structure of a concrete factory floor). The plot starts with $\epsilon'_{rc} = 6.25$ and $p = 0.05$, which we consider as characteristic of sound concrete in the floor of the factory. The three curves prove the same: as porosity increases, ϵ'_{rc} decreases, having a value of 4–5 for a porosity of 20–25%. It is necessary to know how this variation on ϵ'_{rc} from 6.25 to 4–5 affects the radar signal, particularly the reflection in the air–concrete interface.

2.2. Influence of concrete dielectric constant variation in the reflected pulse from the air–concrete interface

The amplitude reflection coefficient at the interface of two materials depends on the electrical prop-

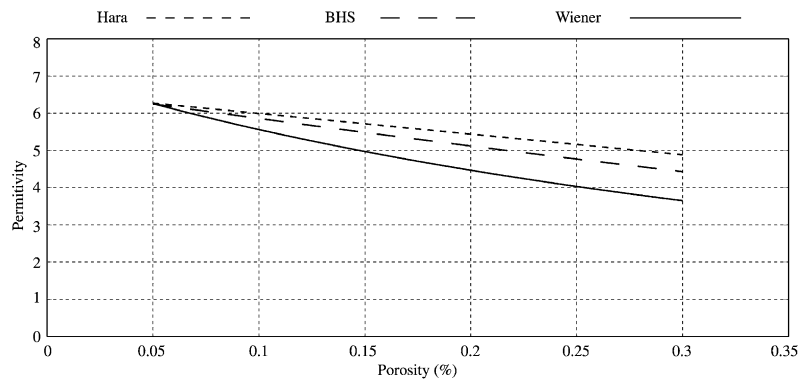


Fig. 2. Real part of relative permittivity of the concrete floor as function of its porosity.

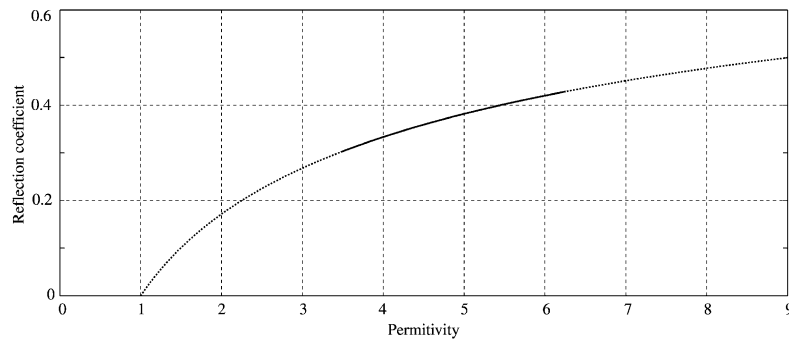


Fig. 3. Amplitude reflection coefficient as function of ϵ'_r at 900-MHz frequency and $\sigma = 10^{-3}$ mho/m.

erties of both of them. It can be expressed as a function of their impedance contrast:

$$r = \frac{\eta_c - \eta_a}{\eta_c + \eta_a} \quad (4)$$

where r = amplitude reflection coefficient, η_a = impedance of air, η_c = impedance of concrete.

Accepting a low level of conductivity for the concrete and taking the electrical properties of air into account, Fig. 1 permits to attain the expression of the reflection coefficient as a function of the permittivity of concrete according to Eq. (5) and Fig. 3:

$$r = \frac{1 - \sqrt{\epsilon'_{rc}}}{1 + \sqrt{\epsilon'_{rc}}} \quad (5)$$

The conclusion of the theoretical study is that, in the very special circumstances of the textile factory floor, it is possible to expect a diminution on the amplitude of radar reflected pulse from degraded areas.

3. Identification of degraded zones

Fig. 4 is a plan-view map of the factory hall. It is organised in corridors 20-m long and 2–3-m wide with the machinery situated between the corridors like the one shown in Fig. 5. A 900-MHz centre frequency monostatic antenna was used in the investigation of the floor because of its good resolution, small dimensions and short pulse emission. A non-metallic skate was designed to move the antenna at a constant distance of 25 cm from the surface. This

was designed to filter the direct signal between dipoles of the antenna for a better identification of reflection from the surface of the concrete floor.

Radar grams were attained moving the antenna at a slow velocity of 0.5 m/s and storing data at 16 scans/s. The results were averaged in order to have homogeneous profiles of 20 scans/m, 1 scan/5 cm, enough horizontal resolution so as degradation of concrete would appear in longer distances.

3.1. Proposed method

Because the filtering action was from the top to the bottom of the concrete layer, it was possible to assume for a high degradation in the first centimeters of the floor. Thus, the first reflection—from air–concrete interface—should be representative of the state of concrete at that point. Fig. 6 is an example of a scan obtained in the factory; the pulse from the top of the floor is highlighted.

For the analysis of amplitude reflection, an automatic calculus program was developed with the following steps:

1. Data reading
2. Filtering of direct signal between dipoles
3. Obtaining of filter data
4. Scan analysis:
 - (a) Definition of *integration limits*
 - (b) Estimation of reflected energy through calculated curve area defined in (a)
5. Obtaining an *attenuation index* (AI, dB) at each point, like the relationship between area attained at this point compared with area attained in a zone of sound concrete

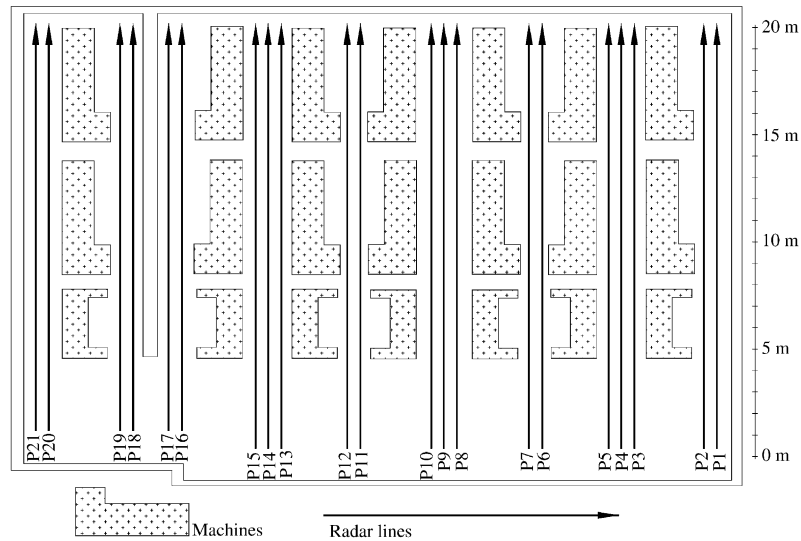


Fig. 4. Plan-view map of the factory hall with the GPR lines carried out in this study.

6. Plot of *attenuation index* at each point of profiles studied
7. These graphs need a final interpretation, which takes into account the effect of local elements in the surface or close to the antenna.

Fig. 7 contains the integrated area of the stored scan of Fig. 6. The selection of those limits is quite subjective; we think it is necessary to study an integration limit large enough to take into account the full reflected pulse from the air–floor interface, but small enough to allow for the influence of external reflections due to the machinery of the factory.

The selection of the integration limits was made taking into account the time length and waveform of the emitted pulse (a “1 1/2 period” pulse, 2 ns timespan, of the 900-MHz antenna used). The first reflection we detected from the air–floor interface was a “2-period” wavelet, which could indicate more than one single reflection. This phenomenon made us think to define the attenuation index as the relationship between “areas” under the reflected pulse instead of its definition using the maximum amplitude of the first 1 1/2 period. We could not make profiles very close to the machines because these reflections appear at the same time that the first reflection from



Fig. 5. One of the corridors of the factory showing the machinery.

the floor surface (we moved our antenna with a skate at 25 cm distance from the floor). This was one more determining factor in the selection of the integration limits: we wanted to take information very close to the machinery but without the influence of these lateral reflections. So, if we wanted to pass near the machines, we had to select the shortest integration limit we could, but long enough to be representative of the pulse reflected on the floor.

The attenuation index will give positive values in cases that examine concrete which has a significantly higher porosity than the reference sound concrete. In this study, we accept that high porosity means deterioration so we can expect positive values from degraded zones. We would like to point out the necessity of careful interpretation of the curves; the presence of local reflectors can mask reflections of the concrete. For example, when the antenna passes over a cable or a metallic plate, the automatic program plots its effect as a large diminution in the attenuation index, but obviously, it has no connec-

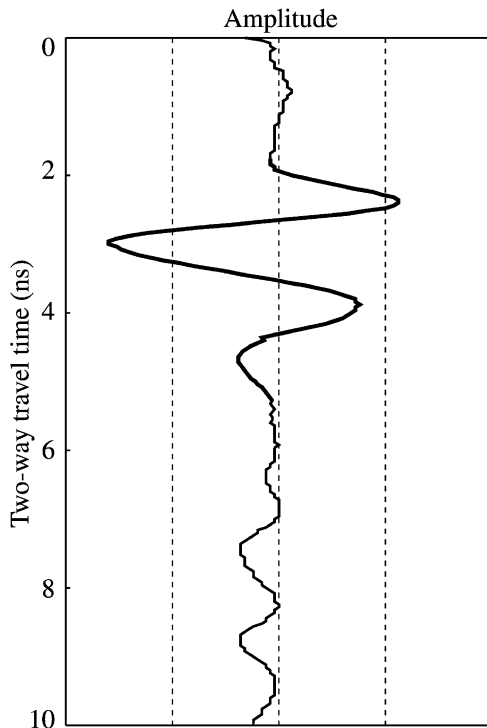


Fig. 6. Example of scan recorded. The highlighted line is the reflection from the top of the floor.

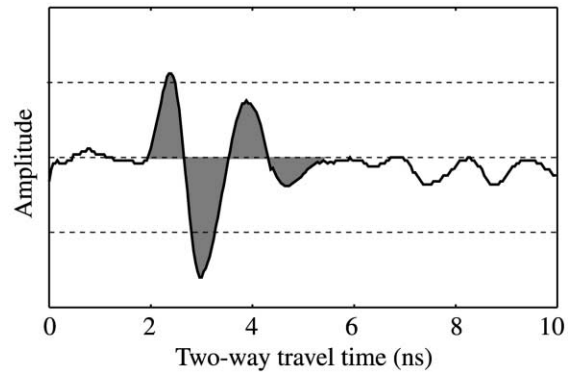


Fig. 7. Integrated lap considered in the calculation of the attenuation index.

tion with the porosity of concrete. We also have found systematic *sine curve* variations of 0.1–0.2 dB along all the profiles we made; these oscillations seem to be caused by the transversal girders inside the floor and also to the effect of concrete rebars.

4. Work field and results

The fieldwork, 21 radar lines (Fig. 4), was carried out in 1 day, without obstructing the factory production process. This was organised in 2–3 profiles of 20 m in each corridor trying not to pass too close to the machinery in order to prevent lateral reflections. The spillage of chemical liquid onto the floor of the corridors started at 10 m of the profiles, but it was not homogeneous along the whole length of them nor in all of them.

The radar line P7 is shown in Fig. 8. This line passes near where a core sample had been taken which showed a concrete porosity of 25%. The core was situated close to 12 m and in this area, one of the biggest attenuation indexes was detected. It is necessary to pay attention to some systematic local *lows* that appear all along the graph; it was possible to associate most of them with the presence of girders situated transversely to the movement of the antenna. Girders crossed radar line at 1.5, 4, 6.5, 11, 13.5, 16 and 19 m, and the presence of some, but not all of them, are distinguishable in the graph.

Before crossing 9.5–10 m, the attenuation index stays close to zero dB, i.e., with similar reflection coefficient to that of sound concrete. After crossing

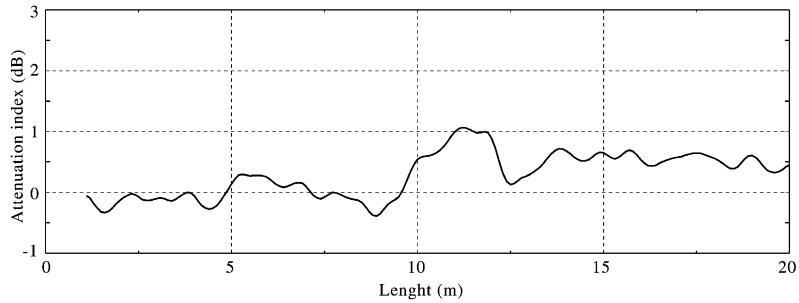


Fig. 8. Attenuation curve of a corridor with evidence of concrete degradation from 10 m; the core drill sample extracted at 12 m had a porosity of 25%. At 1.5, 4, 9, 13 and 19 m, there is local diminution of the attenuation index caused by crossing over transversal girders.

10 m, it is possible to appreciate a global tendency of the curve to increase until 0.5 dB of attenuation index, which indicates an increase of porosity from this point until the end of the profile. The simplicity of the model used does not allow for an accurate estimation of the porosity of concrete at these points, but it permits to give a semi-quantitative idea of which zones of the concrete appear to be affected by the spillage. In order to give an idea of the sensitivity level of the measurement process in relationship with the attenuation index, the theoretical evolution of the porosity of a concrete with a very homogeneous internal structure and with typical parameters: porosity $p = 5\%$ and permittivity $\epsilon'_r = 6.25$, applying the three formulas used in this study, give the following values:

$$\begin{aligned} \text{For AI} = 1 \text{ dB} &\rightarrow \epsilon'_r = 4.1 \rightarrow p = 23.8\% \\ (\text{Wiener}), p &= 34.7\% (\text{Hara}), p = 28.7\% (\text{BHS}) \\ \text{For AI} = 0.5 \text{ dB} &\rightarrow \epsilon'_r = 5 \rightarrow p = 14.6\% \end{aligned}$$

$$\begin{aligned} (\text{Wiener}), p &= 21.4\% (\text{Hara}), p = 18\% (\text{BHS}) \\ \text{For AI} = 0.1 \text{ dB} &\rightarrow \epsilon'_r = 5.95 \rightarrow p = 6.9\% \\ (\text{Wiener}), p &= 8.6\% (\text{Hara}), p = 7.7\% (\text{BHS}) \end{aligned}$$

Fig. 9 is the attenuation graph of radar line P11. The core sample taken near 12 m had a porosity of 15%, while attenuation index is about 0.5 dB after 9–10 m. If we compare the results of the attenuation index graphs with the porosity of the two core drill samples extracted near P5 and P11, we find $\text{AI} = 1 \text{ dB}$ in the zone where a sample of 25% porosity had been taken, and $\text{AI} = 0.5 \text{ dB}$ in the zone where a sample of 15% porosity had been taken. Wiener formula appears to give a good prediction of porosity in this study, but we are sure that the internal structure of the floor is more complex than the model that we used. We believe this model points out changes in porosity because they are quite large (0.5 dB) and they appear over large intervals in some of the radar lines made in the corridors, which allow

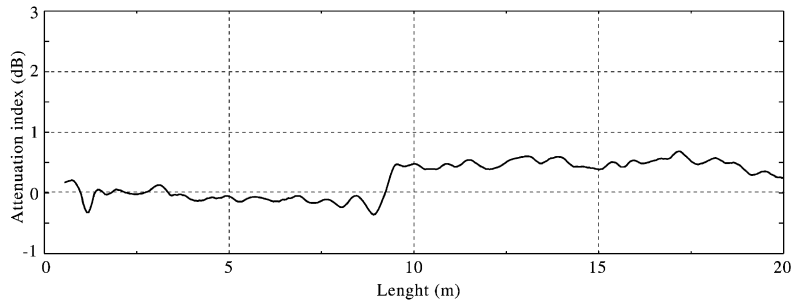


Fig. 9. Attenuation curve of a corridor with evidences of concrete degradation from 10 m. The effect of transversal girders is distinguishable only at 1.5 and 9 m.

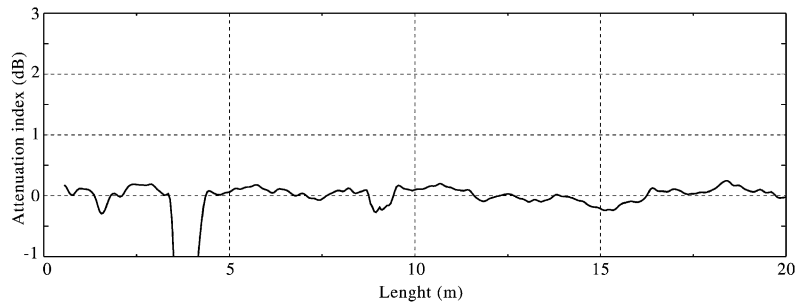


Fig. 10. Attenuation curve of a corridor without signs of large concrete degradation. Index diminutions of 3.5–4 and 9 m are due to the presence of a metal plates and a set of cables.

us to recognize its global effect in the reflected pulses over the local effect of girders and rebars. The graph of radar line P11 shows a response very similar to line P5 (Fig. 8) but seems to have less influence because of transversal girders. The change of the properties of concrete before and after 10 m is clear, with a typical value of about 0.5 dB of attenuation index for the last 10 m, which would mean a porosity in the order of 15% based on the information of the core sample of 12 m.

Not all the corridors of the factory seem to be affected equally by the spillages. Radar line P14 (Fig. 10) is an example of the graphs obtained in

these corridors, where no evidence of high degradation was found along the corridor (the effect of crossing a metal plate and a group of cables appear in 3.5–4 and 9 m, as graph decreases). The systematic oscillations of 0.1–0.2 dB are also present in the graph, but there is no global increase of the curve, which could be related with large porosity changes. We honestly cannot confirm that there is no porosity increase in these corridors because it would be in the order of 0.1–0.2 dB, the same as the systematic variations detected, but porosity increase—if it exists—would not be so high as in the other corridors. Finally, we summarize the results obtained in this

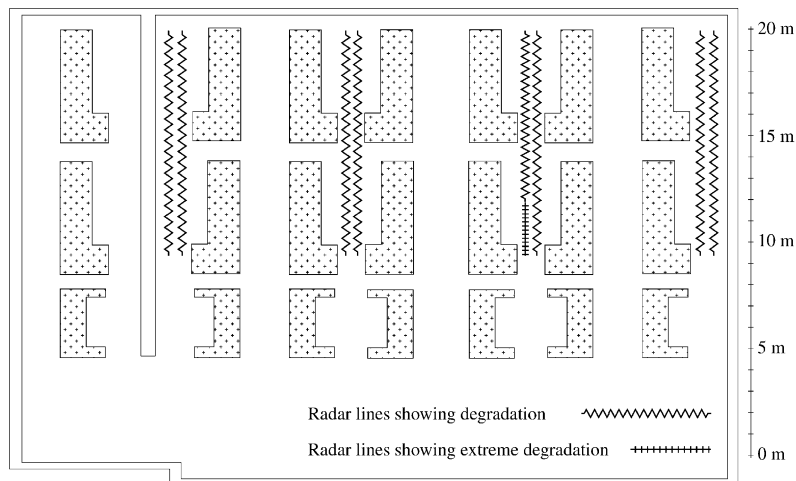


Fig. 11. Plan-view map of the factory hall showing the areas where attenuation index is in the order of 0.5 dB (^^^^^^) and close to 1 dB (++++).

study in Fig. 11, which is a plan-view map of the factory showing the global evolution of the attenuation index obtained.

5. Conclusions

The present work proposes a simple method for the study of concrete deterioration in a factory floor. In this case, deterioration appears as an increase in concrete porosity, which can be detected studying the reflection coefficient of the air–concrete interface.

The concrete was isolated from spillages some years ago, hence, it was possible to accept it as being dry. In this situation, concrete impedance mainly depends on permittivity variation due to porosity changes, and permittivity decreases if porosity increases. So, it is possible to expect a diminution of the reflection coefficient of the air–concrete interface in degraded areas.

The method was applied to areas in which two core drill samples had been extracted, showing different responses in the reflection coefficient depending on core porosity. So, a comprehensive study was carried out, detecting degraded areas of the factory floor.

Acknowledgements

Ground penetrating radar equipment used in the done study is the property of *Laboratorio de Geotecnia* of *Centro de Estudios y Experimentación de Obras Públicas* of Spain.

References

- Al-Qadi, I.L., Loulizi, A., Lahouar, S., 2000. Dielectric characterization of hot-mix asphalt at the smart road using GPR. In: Noon, D.A., Stickley, G.F., Longstaff, D. (Eds.), Eighth International Conference on Ground Penetrating Radar, Queensland, Australia. SPIE, 4084, pp. 176–180.
- Carter, C.R., Chung, T., Masliwec, T., Manning, D.G., 1992. Analysis of radar reflections from asphalt covered bridge deck structures. In: Ground Penetrating Radar, Geological Survey of Canada, Paper 90-4, pp. 33–40.
- Chung, T., Carter, C.R., Masliwec, T., Manning, D.G., 1994. Impulse radar evaluation of concrete, asphalt and waterproofing membrane. IEEE Transactions on Aerospace and Electronic Systems 30 (2), 404–415.
- Cook, J.C., 1975. Radar transparencies of mine and tunnel rocks. Geophysics 4 (5), 865–885.
- Duke, S.K., 1990. Calibration of ground penetrating radar and calculation of attenuation and dielectric permittivity versus depth. MS Thesis, Colorado Scholl of Mines, 236 pp.
- Glover, J.M., 1987. The use of sub-surface radar for shallow site investigation. PhD Thesis, Kings College, University of London, 451 pp.
- Halabe, U.B., 1990. Conditions assessment of reinforced concrete structures using electromagnetic waves. PhD Thesis, Department of Civil Engineering, Massachusetts Institute of Technology, 135 pp.
- Halabe, U.B., Cheng, H.L., Bhandarkar, V., Sami, Z., 1997. Detection of sub-surface anomalies in concrete bridges decks using ground penetrating radar. ACI Materials Journal 94, 396–408.
- Hara, T., Sakayama, T., 1984. The applicability of ground probing radar to site investigations: OYO technical note, 38 pp.
- Lázaro-Mancilla, O., Gómez-Treviño, E., 2000. Ground penetrating radar inversion in 1-D: an approach for the estimation of electrical conductivity, dielectric permittivity and magnetic permeability. Journal of Applied Geophysics 43 (2–4), 199–213.
- Molineaux, T.C.K., Millard, S.G., Bungey, J.H., Zhou, J.Q., 1995. Radar assessment of structural concrete using neural networks. NDT and Evaluation International 28 (5), 281–288.
- Maser, K.R., Scullion, T., 1991. Automated detection of pavement layer thicknesses and subsurface moisture using ground penetrating radar. TRB paper.
- Matthews, S., Goodier, A., Massey, S., 1998. Permittivity measurements and analytical dielectric modelling of plain structural concretes. Seventh International Conference on Ground Penetrating Radar, Lawrence, May 27–30. Radar Systems and Remote Sensing Laboratory, University of Kansas, Kansas, USA, pp. 363–368.
- Olhoft, G.R., 1987. Electrical Properties from 10^{-3} to 10^9 Hz—physics and chemistry. Proceedings of the Second International Symposium on the Physics and Chemistry of Porous Media. Schumberger-Doll, Ridgefield, CT, pp. 281–298.
- Olhoft, G.R., 2000. Automatic processing and modeling of GPR data for pavement thickness and properties. Eighth International Conference on Ground Penetrating Radar. Queensland, Australia, pp. 188–193.
- Reppert, P.M., Morgan, F.D., Toksöz, M.N., 2000. Dielectric constant determination using ground-penetrating radar reflection coefficients. Journal of Applied Geophysics 43 (2–4), 189–197.
- Robert, A., 1998. Dielectric permittivity of concrete between 50 MHz and 1 GHz and GPR measurements for building materials evaluation. Journal of Applied Geophysics 40, 89–94.
- Saarenketo, T., Roimela, P., 1998. Ground penetrating radar technique in asphalt pavement density quality control. Seventh International Conference on Ground Penetrating Radar, Lawrence, May 27–30. Radar Systems and Remote Sensing Laboratory, University of Kansas, Kansas, USA, pp. 461–466.

- Shang, J.Q., Umana, J.A., Bartlett, F.M., Rossiter, J.R., 1999. Measurement of complex permittivity of asphalt pavement materials. *Journal of the Transportation Engineering*, 347–356.
- Shaw, M.R., Millard, S.G., Houlde, M.A., Austin, B.A., Bungey, J.H., 1993. A large diameter transmission line for the measurement of the relative permittivity of construction materials. *British Journal of NDT* 35 (12), 696–704.
- Shaw, M.R., Molineaux, T.C.K., Millard, S.G., Bungey, J.H., 2000. Automatic analysis of GPR scans on concrete structures. In: Noon, D.A., Stickley, G.F., Longstaff, D. (Eds.), *Eighth International Conference on Ground Penetrating Radar*, Queensland, Australia. SPIE, 4084, pp. 449–453.
- Sousky, N.S., Martinelli, D., Varadarajan, S.T., Halabe, U.B., 1996. Radar signal interpretation using neural network for defect detection in concrete. *Materials Evaluation*, 393–397.
- Tsiu, F., Matteus, S.L., 1997. Analytical modelling of the dielectric properties of concrete for subsurface radar applications. *Construction and Building Materials* 11 (3), 149–161.
- Ulriksen, C.P., 1982. Application of impulse radar to civil engineering. PhD Thesis, Department of Engineering Geology, Lund University of Technology, 175 pp.
- Weil, G.J., 1992. Non-destructive testing of bridge, highway and airport pavement. *Fourth International Conference on GPR*, Rovaniemi, Finland, June 8–13, pp. 259–266.
- Yelf, R., Carse, A., 2000. Audit of a road bridge superstructure using ground penetrating radar. In: Noon, D.A., Stickley, G.F., Longstaff, D. (Eds.), *Eighth International Conference on Ground Penetrating Radar*, Queensland, Australia. SPIE, 4084, pp. 249–254.